Journal of Physics: Conference Series **1350** (2019) 012089 doi:10.1088/1742-6596/1350/1/012089

Beam commissioning of the demonstrator setup for the superconducting continuous wave HIM/GSI-Linac

M Miski-Oglu[1,2], K Aulenbacher [1,2,3], W Barth [1,2], M Basten[4], C Burandt[1,2], M Busch[4], T Conrad[4], F Dziuba[1,2,3], V Gettmann[1,2], M Heilmann[2], T Kuerzeder[1,2], J List[1,2,3], S Lauber[1,2,3], H Podlech[4], A Rubin[2], A Schnase[2], M Schwarz[4], S Yaramyshev[2]

[1]Helmholtz Institute Mainz, Mainz, Germany
[2]GSI Helmholtzzentrum für Schwerionenforschung
[3]KPH, Johannes Gutenberg-University, Mainz, Germany
[4]IAP Goethe-Universität Frankfurt, Frankfurt, Germany

E-mail: m.miskioglu@gsi.de

,

Abstract. During successful beam commissioning of the superconducting 15-gap Crossbar H-mode (CH) cavity at GSI Helmholtzzentrum für Schwerionenforschung heavy ions up to the design beam energy have been accelerated. The design acceleration gain of 3.5 MeV inside a length of less than 70 cm has been reached with full transmission for heavy ion beams of up to 1.5 pμA. The measured beam parameters confirm sufficient beam quality. The machine beam commissioning is a major milestone of the R&D for the superconducting heavy ion continuous wave linear accelerator HELIAC (**HE**lmholtz **LI**near **AC**celerator) of Helmholtz Institute Mainz (HIM) and GSI, developed in collaboration with IAP Goethe-University Frankfurt (GUF). The next step is the procurement and commissioning of the so called "Advanced Demonstrator" – the first of four cryomodules for the entire accelerator HELIAC. Results of further Demonstrator beam tests, as well as the status of the "Advanced demonstrator" project will be reported.

1. INTRODUCTION

The design and construction of continuous wave (cw) high intensity Linacs is a crucial goal of worldwide accelerator technology development [1]. In the low- and medium-energy range, cw-Linacs can be used for several applications, as **A**ccelerator **D**riven subcritical nuclear reactor **S**ystems (ADS) [2; 3], synthesis of **S**uper **H**eavy **E**lements (SHE) [4] and material science. In particular the increased projectile intensity, preferably in cw mode, would remarkably improve the SHE yield. The compactness and energy efficiency of such cw facilities requires the use of superconducting (sc) elements in modern high intensity ion linacs [5–9]. For this purpose the heavy ion superconducting (sc) cw linac HELIAC is developed at GSI Helmholtzzentrum für Schwerionenforschung at Darmstadt and Helmholtz Institute Mainz (HIM)[10; 11] under key support of Institut für Angewandte Physik (IAP) of Goethe University Frankfurt (GUF) [12; 13].

Table 1 shows the key parameters of the HELIAC. Heavy ion beams with a mass-to-charge ratio up to $A/z = 6$ will be accelerated by twelve multi-gap CH cavities, operated at 216.816 MHz. The HELIAC should serve for physics experiments, smoothly varying the output particle energy from 3.5 to 7.3 MeV/u and simultaneously preserving high beam quality [14].

Table 1. Design parameters of the HELIAC [13].

Mass-to-charge ratio	6
Frequency (MHz)	216.816
Max. beam current (mA)	1
Injection energy (MeV/u)	1.4
Output energy (MeV/u)	3.5 – 7.3
Output energy spread (keV/u)	± 3
SC CH cavities	12

2. BEAM TESTS OF DEMONSTRATOR

Prior the realization of HELIAC, the demonstrator project is accomplished at GSI in collaboration with HIM and GUF. The demonstrator setup is located downstream of the GSI High Charge State Injector [15] (HLI).

The demonstrator comprises a 15 gap sc CH-cavity (CH0) [16] embedded by two superconducting solenoids; all three components are mounted on a common support frame (see Fig. 1). The beam focusing solenoids provide a maximum magnetic fields of 9.3 T with the free beam aperture is 30 mm. Each solenoid consists of a main Nb_3Sn-coil and two compensation coils made from NbTi. The compensation coils reduce stray field to maximum 30 mT at a longitudinal distance 300 mm from the center of the main coil. A 3000 liter Helium reservoir in vicinity of the radiation protection shelter provides 2 weeks of operation for the demonstrator cryostat. The sc CH-cavity were manufactured by Research Instruments (RI). After surface preparation the cavity was delivered to IAP for tests in a vertical cryostat. The first important milestones for the HELIAC project was the rf-test of the CH0 cavity, where the design gradient and quality factor was achieved [17]. After the final assembly of the helium vessel and further high pressure rinsing (HPR) preparation at RI, the cavity was tested again at GSI in a horizontal cryostat. The cavity performance was significantly improved due to an additional HPR treatment. The initial design goals have been exceeded and maximum accelerating gradient of $E_{acc} = 9.6\,MV\,m^{-1}$ at $Q_0 = 8.14 \times 10^8$ has been achieved [18].

Prior to beam commissioning of the cavity, the rf-power couplers were tested and conditioned in a dedicated test resonator [19; 20]. Inside ISO4 class clean room, the power couplers were integrated in the rf-cavity, as well as three frequency tuners, developed at IAP and manufactured at GSI. Furthermore, the CH-cavity and both solenoids were assembled into a string. After leak testing the accelerating string was integrated into the cryostat outside of the clean room. Figure 2 shows the matching beam line equipped with beam instrumentation devices. It includes beam current transformers, Faraday cups, SEM-profile grids, a dedicated emittance meter, a bunch shape monitor and phase probe pickups (beam energy measurements applying time of flight) provide for proper beam characterization behind the demonstrator.

In June 2017, after a short commissioning of the demonstrator setup and matching line and ramp-up time of some days, the CH0-cavity accelerated for the first time heavy ion beam (Ar^{11+}) with full transmission up to the design beam energy of 1.866 MeV/u ($\Delta W_{kin} = 0.5$ MeV/u). For the first beam test the sc cavity provided an accelerating voltage of more than 1.6 MV.

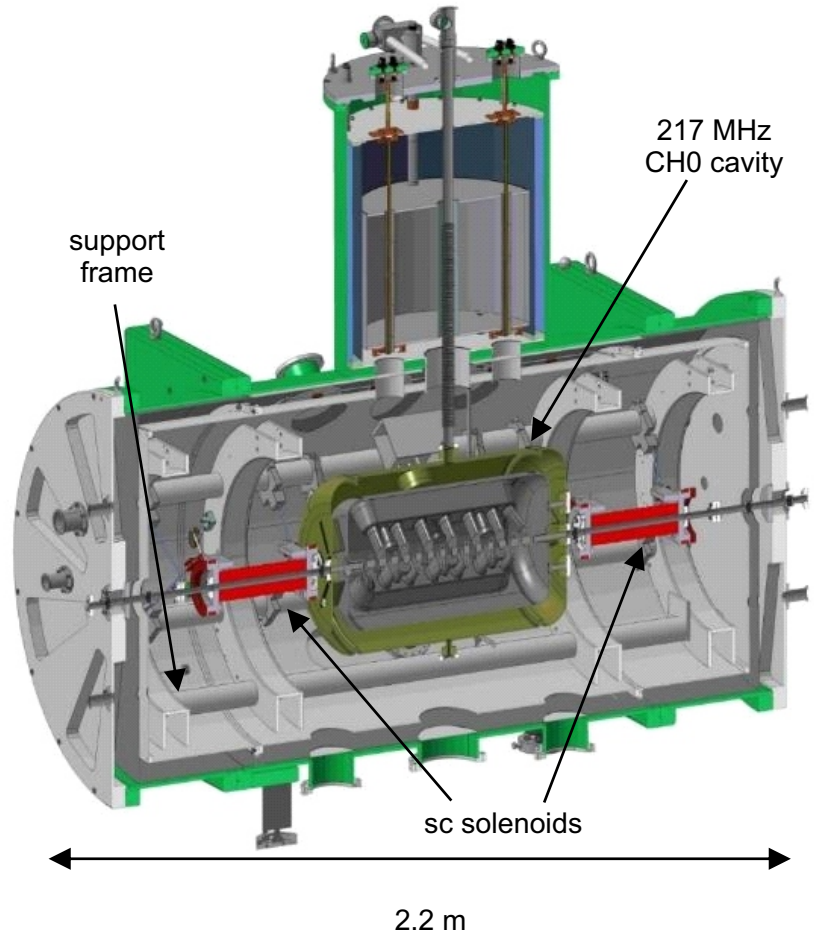

Figure 1. Sectional view of Demonstrator cryostat, the 216.816 MHz CH-cavity and two sc solenoids are suspended within a support frame.

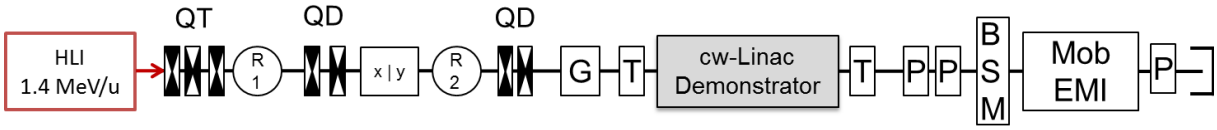

Figure 2. Layout of matching line to the Demonstrator and beam diagnostics test bench. QT/QD=quadrupole triplet/duplet, R = rebuncher, X/Y = beam steerer, G = SEM grid, T = current transformer, P = Phase probe, BSM = bunch shape monitor, EMI = emittance meter.

Furthermore, the design acceleration gain of 3.5 MV has been verified and even exceeded by acceleration of Ar^{6+} beam with higher mass to charge ratio $A/z = 6.7$. A maximum average beam intensity of 1.5 pµA has been achieved, limited only by the beam intensity of the ion source and maximum duty factor (25 %) of the HLI, while the CH-cavity was operated in cw-mode. All presented measurements were accomplished with high duty factor beam and maximum beam intensity from the HLI. A systematic 2-D scan of beam energy and beam transmission for a wide area of different accelerating fields and rf-phases has been performed. The smooth

variation of the beam energy with ramped accelerating gradient could be observed for different rf-phase settings, while the beam transmission was kept above 90 %. Exemplary transversal beam emittance have been measured for accelerated Ar^{9+} beam by a slit grid emittance meter. The measured 90 % emittances in the horizontal and vertical plane are only 0.74 µm and 0.47 µm respectively. The measured (normalized) beam emittance growth at full beam transmission is sufficiently low: 15 % in horizontal plane and 10 % in vertical plane [6]. Besides beam energy measurements the bunch shape was measured with a bunch shape monitor. Impressively small minimum bunch length of about 300 ps (FWHM) and 500 ps (base) could be detected, sufficient for further matching to and acceleration in future rf-cavities

During the beam time in November/December 2018 the result of beam time 2017 were confirmed and further detailed investigation of the longitudinal phase space [21] and further rf-characterization of the CH-cavity [22] were accomplished. Figure 3 shows the measured beam energy (TOF) of the accelerated Ar^{9+} beam as function of the rf-phase for different rf-amplitudes measured at pick-up probe. The measured dissipated power $P_c = P_f - P_r$ in the cavity and quality factor [22] define the stored energy in the cavity. The knowledge of

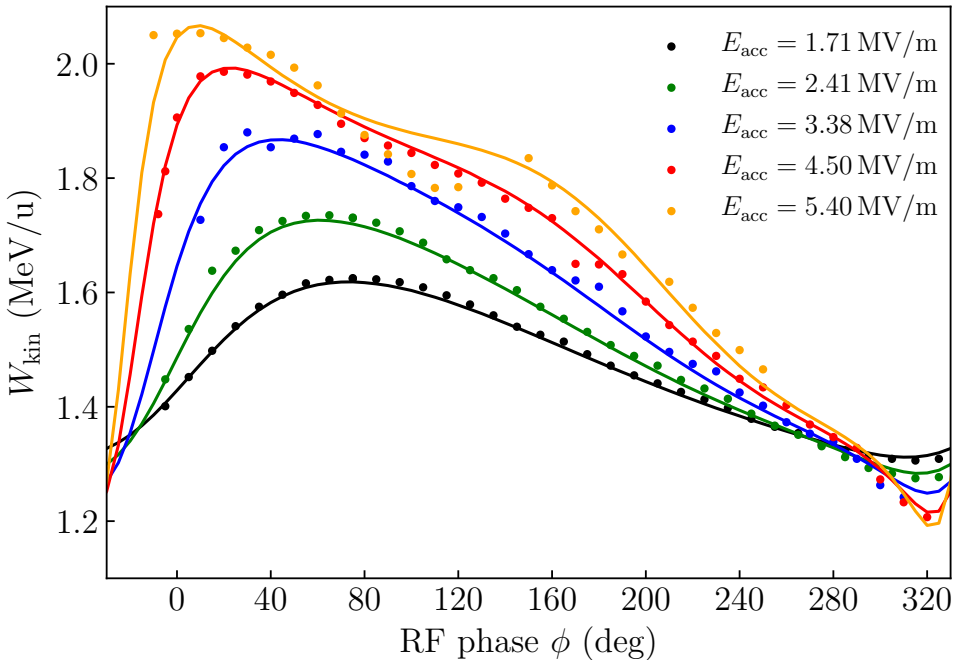

Figure 3. Measured (filled circles) and simulated (solid lines) phase scans for different accelerating gradients.

the stored energy together with the calculated electric field by CST Microwave Studio® [23] (normalized to 1 Joule stored energy) allows assignment of the measured pick-up signal to the unique accelerating gradient. The curves in the Fig. 3 show the calculated kinetic energy gain as function of the cavity phase for different accelerating gradients. The curves are obtained by numerical solution of equation of motion for charged particle in the "real" electric field as exported from CST Microwave Studio®. The agreement of calculated curves with results of TOF measurements confirm the reliability of rf measurements (*i.e.* quality factor) and calibration of the pick-up probe.

3. ADVANCED DEMONSTRATOR

Following the successful beam test of the CH0 cavity within the Demonstrator research project, the next milestone is the construction, commissioning and operation of the Advanced Demonstrator cryomodule. It contains the demonstrator CH0 cavity, two identical CH1 & CH2

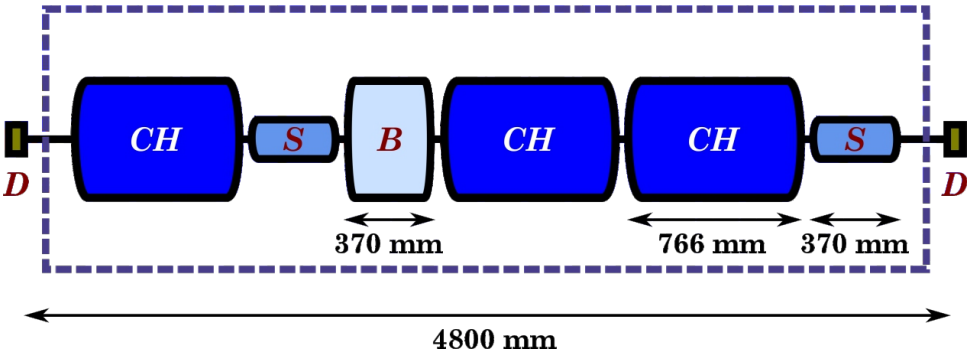

Figure 4. Layout of the Advanced Demonstrator cryomodule containing three CH cavities, a re-buncher cavity (B) and two solenoids (S).

cavities [24], two-gap re-buncher cavity (B) [25; 26] and two sc solenoids (S). Figure 4 shows the layout of the components within the cryomodule. In the future, the Advanced Demonstrator is foreseen to be used as the first of a series of four cryomodules of the HELIAC accelerator. According to beam dynamic simulation [13], the Advanced Demonstrator module will provide for beam energies of up to $W_{kin} = 2.7\,MeV/u$ for heavy ion beams with $A/z = 6$ and up to $W_{kin} = 3.3\,MeV/u$ for lighter beams with $A/z = 3$. The results of rf-testing of CH1 in a vertical cryostat show that design goals are exceeded and a maximum accelerating gradient of $E_{acc} = 9.0\,MV\,m^{-1}$ at $Q_0 = 1.8 \times 10^8$ has been achieved [24]. The CH2 cavity is just before rf-testing in a vertical cryostat. After the final preparation steps by vendor and assembly of the helium jacket, both cavities would be delivered to GSI for the final acceptance rf-tests. The two-gap re-buncher cavity is already designed; the procurement of the Nb material has been started.

Figure 5 shows the 3-D model of the Advanced Demonstrator cryostat. All components will be cleaned and added to the accelerator string within a ISO4 clean room [27] at HIM. After the vacuum leak test, the string is integrated into the cryostat outside the clean room. The large service doors of the cryostat allow easy assembly of the "cold" and "warm" parts of the power couplers after integration of the accelerator string into the cryostat. Moreover, it allows the *in situ* alignment to the beam axis after installation of the cryomodule in the tunnel for each individual component. The newly build Advanced Demonstrator testing area at GSI provides an enlarged radiation protection shelter, the connection to the cryo plant via dedicated Helium distribution valve box, a new rf gallery equipped with four 3 kW rf- amplifiers and a new control room.

4. CONCLUSION

In the future the existing UNILAC (**UNI**versal **L**inear **A**ccelerator) [28–31] at GSI will be exclusively used as an injector for FAIR to provide short-pulse high-intensity heavy ion beams at low repetition rates [32–35]. The new superconducting heavy ion Linac HELIAC(see fig. 6) should provide ion beams above the Coulomb barrier to ensure the GSI SHE program remains competitive world wide. The Linac design comprises a room temperature cw injector, low energy beam transport (LEBT) section followed by a sc Drift Tube Linac (DTL) consisting of 12 sc CH

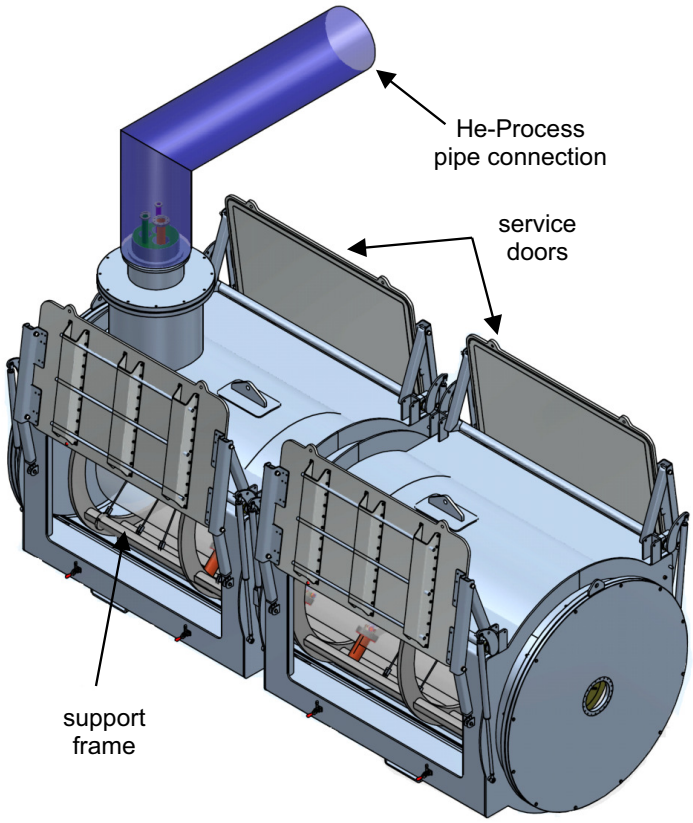

Figure 5. 3-D model of the Advanced Demonstrator cryo module.

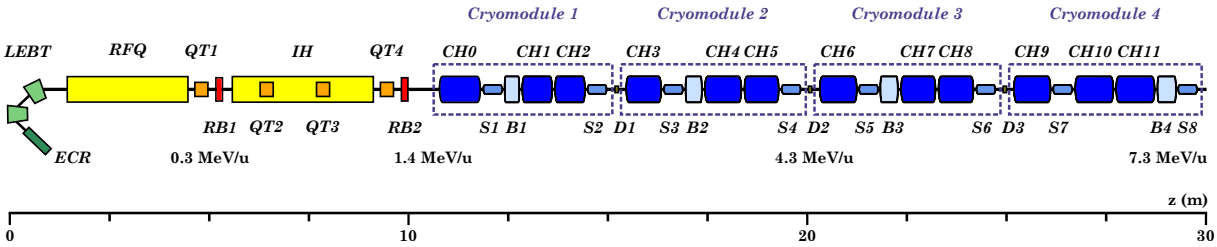

Figure 6. Layout of the HELIAC accelerator.

structures grouped into four cryomodules (CM1-CM4). Besides acceleration of the design ions the HELIAC can be operated with different ions from protons ($A/z = 1$) to U^{28+} ($A/z = 8.5$). From the beam dynamics point of view, an output energy of up to 10 MeV/u for light ions (14 MeV for protons) could be reached without significant performance degradation.

References

[1] Prior C R 2010 *Proc. HB'10, Morschach, Switzerland, Sep.-Oct. 2010* pp 6–10
[2] Wang Z J *et al.* 2016 *Phys. Rev. Accel. Beams* **19**(12) 120101
[3] Polozov S M and Fertman A D 2013 *Atomic Energy* **113** 192–200
[4] Khuyagbaatar J a 2014 *Phys. Rev. Lett.* **112** 172501

[5] Mardor I *et al.* 2018 *EPJ A* **54** 91
[6] Barth W *et al.* 2018 *Phys. Rev. Accel. Beams* **21**(2) 020102
[7] Sakamoto N *et al.* 2018 *Proc. LINAC'18, Beijing, China, 16-21 September* (Geneva, Switzerland: JACoW) pp 620–625
[8] Ostroumov P *et al.* 2018 *Proc. IPAC'18, Vancouver, BC, Canada, April 29-May 4* (Geneva, Switzerland: JACoW Publishing) pp 2950–2952
[9] Conway Z *et al.* 2018 *Proc. SRF'17, Lanzhou, China, July 17-21* (Geneva, Switzerland: JACoW) pp 692–694
[10] Barth W *et al.* 2018 *J. Phys. Conf. Ser.* **1067** 052007
[11] Yaramyshev S *et al.* 2018 *J. Phys. Conf. Ser.* **1067** 052005
[12] Podlech H *et al.* 2007 *Phys. Rev. ST Accel. Beams* **10**(8) 080101
[13] Schwarz M *et al.* 2018 *J. Phys. Conf. Ser.* **1067** 052006
[14] Barth W *et al.* 2017 *EPJ Web Conf.* **138** 01026
[15] Gerhard P *et al.* 2010 *Proc. IPAC'10, Kyoto, Japan, May*
[16] Dziuba F *et al.* 2010 *Phys. Rev. ST Accel. Beams* **13**(4) 041302
[17] Dziuba F *et al.* 2017 *Proc. LINAC'16, East Lansing, MI, USA, 25-30 September* (Geneva, Switzerland: JACoW) pp 953–955
[18] Dziuba F *et al.* 2017 *Proc. RuPAC'16, St. Petersburg, Russia, November 21-25* (Geneva, Switzerland: JACoW) pp 83–85
[19] Busch M *et al.* 2017 *Proc. LINAC'16, East Lansing, MI, USA, 25-30 September* (Geneva, Switzerland: JACoW) pp 913–915
[20] List J *et al.* 2019 *Proc. LINAC'18, Beijing, China, 16-21 September* (Geneva, Switzerland: JACoW) pp 920–923
[21] Lauber S *et al.* 2019 *presented at IPAC'19, Melbourne, Australia, May 2019*
[22] Dziuba F *et al.* 2019 *presented at IPAC'19, Melbourne, Australia, May 2019*
[23]
[24] Basten M *et al.* 2019 *Proc. LINAC'18, Beijing, China, 16-21 September* (Geneva, Switzerland: JACoW) pp 855–858
[25] Gusarova M *et al.* 2018 *J. Phys. Conf. Ser.* **1067** 082005
[26] Taletskiy K *et al.* 2018 *J. Phys. Conf. Ser.* **1067** 082006
[27] Kuerzeder T *et al.* 2019 *presented at IPAC'19, Melbourne, Australia, May 2019*
[28] Barth W *et al.* 2015 *Phys. Rev. ST Accel. Beams* **18**(4) 040101
[29] Adonin A A *et al.* 2014 *Rev. Sci. Instrum.* **85** 02A727
[30] Yaramyshev S *et al.* 2006 *Nucl. Instrum. Methods Phys. Res. Sect. A* **558** 90 – 94
[31] Barth W *et al.* 2007 *Nucl. Instrum. Methods Phys. Res. Sect. A* **577** 211 – 214
[32] Barth W *et al.* 2017 *Phys. Rev. Accel. Beams* **20**(5) 050101
[33] Barth W *et al.* 2015 *Phys. Rev. ST Accel. Beams* **18**(5) 050102
[34] Groening L *et al.* 2008 *Phys. Rev. ST Accel. Beams* **11**(9) 094201
[35] Yaramyshev S *et al.* 2015 *Phys. Rev. ST Accel. Beams* **18**(5) 050103